# Regulation of inositol 1,4,5-trisphosphate-induced $Ca^{2+}$ release. I. Effect of $Mg^{2+}$

POMPEO VOLPE, BARBARA H. ALDERSON-LANG, AND G. ALLEN NICKOLS
*Departments of Physiology and Biophysics and of Pharmacology and Toxicology, University of Texas Medical Branch, Galveston, Texas 77550*

VOLPE, POMPEO, BARBARA H. ALDERSON-LANG, AND G. ALLEN NICKOLS. *Regulation of inositol 1,4,5-trisphosphate-induced $Ca^{2+}$ release. I. Effect of $Mg^{2+}$*. Am. J. Physiol. 258 (Cell Physiol. 27): C1077–C1085, 1990.—Canine cerebellar membranes were fractionated by differential centrifugation into a crude mitochondrial pellet ($P_2$) and a crude microsomal pellet ($P_3$). The effect of $Mg^{2+}$ on inositol 1,4,5-trisphosphate ($IP_3$)-induced $Ca^{2+}$ release and [$^3$H]$IP_3$ binding was assessed. $Mg^{2+}$ inhibited $IP_3$-induced $Ca^{2+}$ release in a concentration-dependent manner. $Mg^{2+}$ influenced both the extent of $IP_3$-induced $Ca^{2+}$ release and the apparent affinity for $IP_3$. A 10-fold change of free $Mg^{2+}$ (from ~30 to ~300 $\mu$M) reduced the extent of $Ca^{2+}$ release by two- to threefold and shifted the apparent Michaelis constant from ~0.5 to ~0.9 $\mu$M $IP_3$. Thus $Mg^{2+}$ seemed to be a noncompetitive inhibitor of $IP_3$-induced $Ca^{2+}$ release. $Mg^{2+}$ also inhibited $Ca^{2+}$ release elicited by glycerophosphoinositol 4,5-bisphosphate, a poorly metabolized analogue of $IP_3$. $Mg^{2+}$ and heparin sodium were shown to be additive inhibitors of $IP_3$-induced $Ca^{2+}$ release. $Mg^{2+}$ inhibited [$^3$H]$IP_3$ binding under experimental conditions designed to minimize $IP_3$ hydrolysis. Scatchard plots indicated that 0.5 mM free $Mg^{2+}$ reduced maximum binding from 10.9 to 3.5 pmol $IP_3$ bound/mg protein and increased the dissociation constant from 136 to 227 nM. The modulation of [$^3$H]$IP_3$ binding and $IP_3$-induced $Ca^{2+}$ release by $Mg^{2+}$ could be physiologically relevant.

magnesium; calcium channel

REDISTRIBUTION OF INTRACELLULAR $Ca^{2+}$ is a key event in cell activation. The belief that neurotransmitters (20), hormones, agonists, and growth factors act at plasma membrane receptors to stimulate the breakdown of phosphatidylinositol 4,5-bisphosphate into diacylglycerol and inositol 1,4,5-trisphosphate ($IP_3$) is widely accepted (for a review, see Ref. 3). $IP_3$ has been shown to be the link between receptor activation and $Ca^{2+}$ release from intracellular store(s) (3). The ability of $IP_3$ to act as an intracellular messenger has been described in a large number of cell types (3), including neurons and model neurotumor cells (11, 20). Hydrolysis of phosphatidylinositol 4,5-bisphosphate might serve a number of functions in nerve cells, e.g., excitability, secretion of neurotransmitters, posttetanic potentiation, and differentiation. The physiological role of $IP_3$-induced $Ca^{2+}$ release in nerve cells remains to be fully elucidated.

Isolated membrane fractions have been used to investigate several aspects of the mechanism of $IP_3$-induced $Ca^{2+}$ release. Membrane fragments derived from the cerebellum display a very high density of $IP_3$ binding sites (27) and have quickly become a useful model to study properties and regulation of $IP_3$-induced $Ca^{2+}$ release (1, 15, 16, 24, 25).

In this and in the accompanying paper (26), we have investigated the roles of $Mg^{2+}$ and adenosine 3′,5′-cyclic monophosphate-dependent protein kinase in $IP_3$-induced $Ca^{2+}$ release from canine cerebellar membrane fragments. $Mg^{2+}$ is shown to be a noncompetitive inhibitor of $IP_3$-induced $Ca^{2+}$ release and [$^3$H]$IP_3$ binding. Thus the resting free $Mg^{2+}$ concentration as well as transient or long-lasting changes of intracellular free $Mg^{2+}$ might influence the open-closed state of the $IP_3$-gated $Ca^{2+}$ channel.

## MATERIALS AND METHODS

*Isolation of crude mitochondrial and crude microsomal pellet fractions from canine cerebellum.* Brains were obtained from mongrel dogs of either sex weighing 10–15 kg. The dogs were anesthetized by intravenous injection of a mixture of $\alpha$-chloralose (0.1 g/kg) and urethan (1 g/kg) and were later killed with a lethal dose of the anesthetic mixture. Immediately after exsanguination, the skull was opened with the use of an osteotome, and the meninges surrounding the brain were cut away. The cerebellum was removed from the brain and immediately sealed in a plastic bag on ice from which it was transferred to a −80°C freezer and stored until needed.

The procedure used for isolating the crude mitochondrial pellet ($P_2$) and crude microsomal pellet ($P_3$) was based on the procedure of Edelman et al. (9) with a few minor modifications as outlined by Alderson and Volpe (1). Briefly, the cerebellums were initially homogenized in 10 vol of ice-cold *buffer A* [0.32 M sucrose, 5 mM *N*-2-hydroxyethylpiperazine-*N*′-2-ethanesulfonic acid (HEPES), 0.1 mM phenylmethylsulfonyl fluoride, pH 7.4]. After the first spin at 900 *g*, the pellets ($P_1$) were resuspended in 5 vol of *buffer A* and homogenized again. The supernatants ($S_1$) collected from the first and second centrifugation steps were poured through six layers of cheesecloth before the 17,000 *g* spin from which the $P_2$ fractions were obtained. $P_3$ fractions were obtained by centrifugation of $S_2$ supernatants at 100,000 *g*. All centrifugations were carried out at 4°C. The $P_2$ and $P_3$ fractions were resuspended and rehomogenized by a hand-held glass-Teflon homogenizer in a small volume of *buffer A* and stored in 0.5- to 1.0-ml aliquots in liquid nitrogen until used. Previously (1), $P_2$ and $P_3$ fractions

 

were found to have similar levels of [$^3$H]$IP_3$ binding and to differ markedly in the extent of $IP_3$-induced $Ca^{2+}$ release. Most of the present experiments were carried out with both membrane fractions to identify the possible cause of such a discrepancy. The protein concentration of each fraction was determined by the Lowry method, using bovine serum albumin as a standard.

*$Ca^{2+}$ uptake and $IP_3$-induced $Ca^{2+}$ release.* $Ca^{2+}$ uptake and $IP_3$-induced $Ca^{2+}$ release were measured as described (1). The assay was carried out at 37°C in a medium containing 40 mM KCl, 62.5 mM potassium phosphate, 8 mM potassium-3-(*N*-morpholino)propanesulfonic acid (MOPS), pH 7.0, 0.04 mg/ml creatine phosphokinase, 0.2 mM phosphocreatine, 1 mM $Na_2ATP$, 0.1–3 mM $MgCl_2$, and 162.5 μM antipyrylazo III, in a final volume of 1 ml. $Ca^{2+}$ fluxes were monitored spectrophotometrically in a Hewlett-Packard 8451A spectrophotometer after the differential absorbance (790–710 nm) of the $Ca^{2+}$-sensitive dye antipyrylazo III. Each fraction (0.5 mg of protein) was added to the uptake-release medium and allowed to equilibrate to 37°C for 10 min. After this, $Ca^{2+}$ was administered in two 10-nmol aliquots. After the administered $Ca^{2+}$ was completely accumulated by the preparation, 0.1–20 μM $IP_3$ was added to the medium. In some experiments, glycerophosphoinositol 4,5-bisphosphate ($GPIP_2$) was used to induce $Ca^{2+}$ release. At the end of each experiment, 10 nM $CaCl_2$ was added to recalibrate the antipyrylazo III response.

The free $Mg^{2+}$ and MgATP concentrations of the uptake-release medium were calculated using a modified computer program ("IONS" or "SPECS") originally designed by Dr. Alexandre Fabiato (Medical College of Virginia, Richmond).

*[$^3$H]$IP_3$ binding.* [$^3$H]$IP_3$ binding was measured using a centrifugation assay as previously described (1). [$^3$H]-$IP_3$ binding was carried out at 1.6°C in a medium containing 50 mM tris(hydroxymethyl)aminomethane (Tris)·HCl, pH 8.3, 100 mM KCl, 1 mM EDTA, in a final volume of 0.5 ml. In those experiments in which the effect of $Mg^{2+}$ on $IP_3$ binding was investigated, the medium composition was modified to contain 50 mM phosphate and specified concentrations of $MgCl_2$. Typically, total [$^3$H]$IP_3$ binding was measured in the presence of 50 nM [$^3$H]$IP_3$, and nonspecific binding was measured in the presence of both 50 nM [$^3$H]$IP_3$ and 5 μM nonradioactive $IP_3$. Specific $IP_3$ binding was determined as the difference between total and nonspecific binding. To obtain Scatchard plots, total [$^3$H]$IP_3$ binding was measured in the presence of 5–300 nM [$^3$H]$IP_3$ only, whereas nonspecific binding was measured in the presence of 5–300 nM [$^3$H]$IP_3$ and corresponding 100-fold concentrations of nonradioactive $IP_3$. From Scatchard analyses, apparent dissociation constants ($K_d$) and maximal binding ($B_{max}$) for [$^3$H]$IP_3$ binding to cerebellar fractions were obtained.

The detailed protocol for the centrifugation assay is outlined in Ref. 1. Briefly, cerebellar fractions were added in a final concentration of 1 mg/ml and incubated in binding media in plastic tubes on ice for 30 min with occasional vortexing. After the 30-min incubation period, 0.43 ml from each $IP_3$ tube of binding medium was transferred to an ultraclear airfuge centrifuge tube that was spun at high speed in a Beckman Airfuge for 10 min at 23°C. The colorless supernatant was carefully removed from the tube after which the pellet was rinsed once with chilled binding buffer not containing $IP_3$. The pellet was solubilized by adding 0.43 ml of 10% (wt/vol) glycerol, 5% (vol/vol) 2-mercaptoethanol, 2.3% (wt/vol) sodium dodecyl sulfate, and 625 mM Tris·HCl, pH 6.8, to the tube and incubating it for a minimum of 3 h. Then the entire tube containing the pellet and solubilizing buffer was placed in a vial containing 15 ml of Opti-Fluor (Packard Bell) scintillation cocktail and analyzed by liquid scintillation spectrometry.

[$^3$H]$IP_2$ binding was carried out as described above using 15 nM [$^3$H]$IP_2$.

*Measurements of [$^3$H]$IP_3$ hydrolysis.* To determine the extent of $IP_3$ hydrolysis occurring, high-pressure liquid chromatography (HPLC) analysis was performed on [$^3$H]$IP_3$ binding media of 0.5 ml vol, consisting of (in mM) 50 Tris buffer, pH 8.3, 1 EDTA, 50 $K_2HPO_4$, and 50 [$^3$H]$IP_3$. Two different types of "control" experiments were designed. One type contained only [$^3$H]$IP_3$ and no added protein or $Mg^{2+}$ to assess the initial level of $IP_3$ hydrolysis in the radioactive sample itself. A second type contained 0.5 mg protein and [$^3$H]$IP_3$ to assess the level of $IP_3$ degradation by the $IP_3$ase present in the protein sample before addition of $Mg^{2+}$. "Experimental media" contained 0.5 mM $MgCl_2$ in addition to 0.5 mg protein and [$^3$H]$IP_3$ and were prepared in Silanized 2-ml centrifuge tubes and incubated on ice for 30 min at 1.6°C. At the end of the incubation period, 0.5 ml of 10% (wt/vol) trichloroacetic acid (TCA) was added to stop the binding reaction.

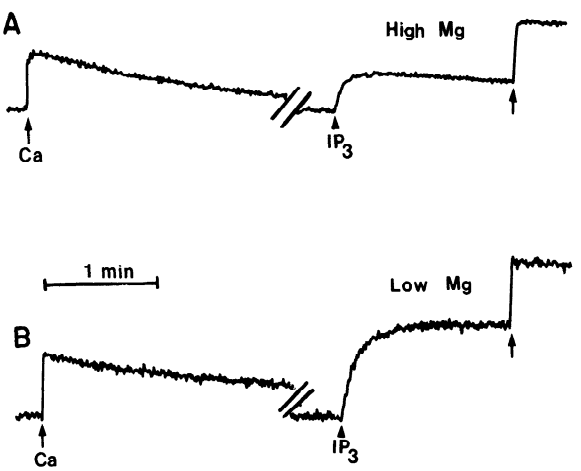


FIG. 1. $IP_3$-induced $Ca^{2+}$ release from cerebellar crude mitochondrial pellet fraction at high (2 mM) and low (0.3 mM) total $Mg^{2+}$. $Ca^{2+}$ loading and $Ca^{2+}$ release were measured as described in MATERIALS AND METHODS using antipyrylazo III as a $Ca^{2+}$ indicator. Assay was started by adding 0.5 mg of membrane protein. Two consecutive 10 nmol $CaCl_2$ pulses were administered (2nd addition is shown at arrow). After completion of $Ca^{2+}$ loading, 10 μM $IP_3$ was added (arrowheads). A downward deflection of absorbance tracing after $Ca^{2+}$ administration is indicative of $Ca^{2+}$ loading, and an upward deflection corresponds to $Ca^{2+}$ release. At end of each experiment, 10 nmol $CaCl_2$ were added to recalibrate antipyrylazo III response (arrows). Data points were stored on Hewlett-Packard microflexible disks, and tracings were electronically scaled so that $Ca^{2+}$ releases are directly comparable. *A*: total $Mg^{2+}$ was 2 mM, and free $Mg^{2+}$ was calculated to be 334 μM; *B*: total $Mg^{2+}$ was 0.3 mM, and free $Mg^{2+}$ was calculated to be 28.6 μM.

TABLE 1. *Effects of $Mg^{2+}$ on $IP_3$-induced $Ca^{2+}$ release from cerebellar $P_2$ and $P_3$*

| | $P_2$ | | $P_3$ | |
|---|---|---|---|---|
| | 0.3 mM $Mg^{2+}$ (28.6 $\mu$M free $Mg^{2+}$) | 2 mM $Mg^{2+}$ (334 $\mu$M free $Mg^{2+}$) | 0.3 mM $Mg^{2+}$ (28.6 $\mu$M free $Mg^{2+}$) | 2 mM $Mg^{2+}$ (334 $\mu$M free $Mg^{2+}$) |
| Rate of $Ca^{2+}$ release, nmol $Ca^{2+}\cdot min^{-1}\cdot mg\ protein^{-1}$ | 228.7±22.9 (8) | 141.9±18.5 (7) | 179.7±21.9 (12) | 106.7±8.8 (7) |
| Extent of $Ca^{2+}$ release, nmol $Ca^{2+}$/mg protein | 30.0±3.4 (8) | 17.1±4.3 (7) | 15.9±3.1 (12) | 6.9±1.1 (7) |
| $K_m$, $\mu$M | 0.48±0.10† (4) | 0.94±0.15† (3) | 0.39±0.11† (4) | 0.88±0.17† (3) |
| Hill coefficient | 1.51±0.16* (4) | 1.63±0.19* (3) | 1.69±0.14* (4) | 1.78±0.20* (3) |

Values are means ± SD of no. of experiments in parentheses. $P_2$, crude mitochondrial pellet; $P_3$, crude microsomal pellet. Experiments were carried out as described in MATERIALS AND METHODS and in legends to Figs. 1 and 3. Rate and extent of $Ca^{2+}$ release were measured in presence of 10 $\mu$M $IP_3$. Michaelis constant ($K_m$) and Hill coefficient were calculated as described in Fig. 3*C*. Relative size of inositol 1,4,5-trisphosphate ($IP_3$)-sensitive and $IP_3$-insensitive $Ca^{2+}$ stores was calculated as follows: total $Ca^{2+}$ accumulated by preparation was 40 nmol $Ca^{2+}$/mg protein and is defined as total $Ca^{2+}$ store ($Tot_{Ca^{2+}}$). $IP_3$ was able to release only part of actively accumulated $Ca^{2+}$. Size of the $IP_3$-sensitive $Ca^{2+}$ store was calculated from (extent of $Ca^{2+}$ release/$Tot_{Ca^{2+}}$) × 100 and was 75 and 43% of total ($IP_3$ sensitive and $IP_3$ insensitive) $Ca^{2+}$ store at low and high free $Mg^{2+}$, respectively (second line, first two columns). * Not significant; † $P < 0.05$.

HPLC analysis was also performed on $Ca^{2+}$ release assay media of 0.5 ml vol containing 40 mM KCl, 52.5 mM potassium phosphate, 8 mM potassium MOPS, pH 7.0, 0.04 mg/ml creatine phosphokinase, 0.2 mM phosphocreatine, 1 mM $Na_2ATP$, and either 0.3 or 2 mM $MgCl_2$. Control media contained no protein, and experimental media contained 0.5 mg protein. The media were prepared in Silanized 2.0-ml centrifuge tubes and incubated at 37°C for 10 min after which 10 $\mu$M $IP_3$ spiked with 0.03 $\mu$Ci [$^3$H]$IP_3$ was added. Twenty seconds after the addition of $IP_3$ to the media, the $Ca^{2+}$ release reaction was stopped with the addition of 0.5 ml of ice-cold 10% (wt/vol) TCA.

After the addition of TCA, the media were vortexed and centrifuged in a Fisher microfuge (model 235A) at high speed for 5 min in a cold room (4°C). The supernatants were extracted five times with ice-cold ethyl ether. After the extractions, the supernatant was run on the HPLC column. Alternatively, the supernatant was frozen at −80°C, lyophilized, and then resuspended in 0.4 ml of 1 mM EDTA, pH 7.0.

The HPLC analysis was carried out using a Du Pont Zorbax SAX column. The samples were eluted in 1-ml fractions by a two-step gradient from 0 to 100% of 0.6 M ammonium formate, pH 3.7 (flow rate, 1 ml/min). After being eluted from the column, the fractions were mixed with Flo-Scint IV scintillation fluid (Packard Bell) at a flow rate of 3 ml/min. They were then passed through an on-line $\beta$-detector (Radiomatic Flo-One model CT) to assess the level of radioactivity in each fraction. The identification of the different inositol phosphates was based on the retention time of labeled standards.

*Materials.* $IP_3$, inositol 1,4-bisphosphate ($IP_2$), $GPIP_2$, HEPES, and MOPS were obtained from Calbiochem; [$^3$H]$IP_3$ and [$^3$H]$IP_2$ from New England Nuclear; $CaCl_2$ and $MgCl_2$ stock solutions, heparin (catalog no. 5640), and antipyrylazo III from Sigma; and ATP from Pharmacia. Ultra-pure grade sucrose was from Schwarz-Mann Biotech. All other chemicals were of analytical or higher grade.

## RESULTS

*$Mg^{2+}$ inhibition of $IP_3$-induced $Ca^{2+}$ release.* In Fig. 1, the cerebellar $P_2$ fraction actively accumulated two consecutive 10-nmol $CaCl_2$ pulses (up to 40 nmol $Ca^{2+}$/mg protein) and then released a certain amount of $Ca^{2+}$ when challenged with 10 $\mu$M $IP_3$ (arrowheads in Fig. 1). As shown in Fig. 1*A* (2 mM total $Mg^{2+}$ and 334 $\mu$M free $Mg^{2+}$), $IP_3$ released ~38.5% of the accumulated $Ca^{2+}$ within ~20 s, and as shown in Fig. 1*B* (0.3 mM total $Mg^{2+}$ and 28.6 $\mu$M free $Mg^{2+}$), $IP_3$ released twice as much $Ca^{2+}$. The rate of $Ca^{2+}$ release was also faster at the lower free $Mg^{2+}$ concentration (see also Table 1). Thus $Mg^{2+}$ interfered with the $Ca^{2+}$-releasing action of $IP_3$.

$Ca^{2+}$-loading rates were similar in both cases (Fig. 1, *A* and *B*) and were at least one order of magnitude lower than $Ca^{2+}$-release rates. Experimental conditions were such that $Ca^{2+}$ loading was carried out at MgATP concentrations of 725 and 185 $\mu$M (Fig. 1, *A* and *B*, respectively), i.e., well above its Michaelis constant ($K_m$) of ~27 $\mu$M.[1] The larger $Ca^{2+}$ release observed in Fig. 1*B* was therefore not likely due to a reduced $Ca^{2+}$ reuptake during release.

Figure 2 shows that $Mg^{2+}$ inhibited $IP_3$-induced $Ca^{2+}$ release from both $P_3$ and $P_2$ fractions (Fig. 2, *A* and *B*, respectively) in a concentration-dependent manner. Half-maximal inhibition of $Ca^{2+}$ release was attained at $Mg^{2+}$ concentrations of 61.2 ± 6.8 and 69.3 ± 7.1 (SD) $\mu$M for $P_3$ and $P_2$ fractions, respectively ($n = 3$).

In Figs. 1 and 2, $Ca^{2+}$ release was elicited by 10 $\mu$M $IP_3$ to counteract the action of $IP_3$ase, which degrades $IP_3$ in a $Mg^{2+}$-dependent fashion (8, 14). The extent of $IP_3$ hydrolysis was measured in $Ca^{2+}$ release media containing 10 $\mu$M [$^3$H]$IP_3$ and either low or high free $Mg^{2+}$ (28.6 and 334 $\mu$M $Mg^{2+}$, respectively). As judged by HPLC chromatograms, after 20 s at 37°C, $IP_3$ comprised 90.6 and 86.4% of the total inositol phosphates at low and high free $Mg^{2+}$, respectively. Thus the concentration of $IP_3$ remaining after 20 s was >8.5 $\mu$M and was still at saturating levels (i.e., >2 $\mu$M; see below Fig. 3*A*).

Figure 3*A* shows that $Mg^{2+}$ reduces the extent of $IP_3$-induced $Ca^{2+}$ release at saturating $IP_3$ concentrations. Figure 3*B* shows the effect of $Mg^{2+}$ on the dose-response curve for $IP_3$-induced $Ca^{2+}$ release when the extent of $Ca^{2+}$ release is replotted as percentage of maximal re-

[1] $K_m$ was calculated from Lineweaver-Burk plots of $1/Ca^{2+}$ loading rate vs. [MgATP]. In the assays, total $Mg^{2+}$ concentration varied from 0.1 to 5 mM and total ATP from 0.1 to 2 mM.

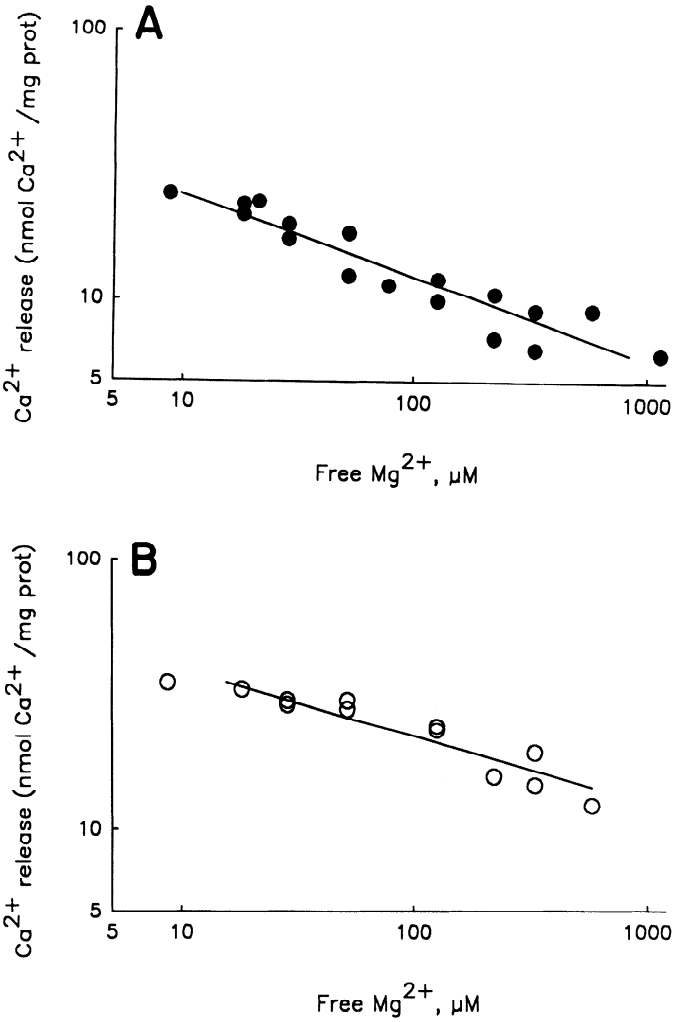


FIG. 2. $Mg^{2+}$ inhibition of $IP_3$-induced $Ca^{2+}$ release from cerebellar crude mitochondrial pellet ($P_2$) and crude microsomal pellet ($P_3$) fractions. $IP_3$-induced $Ca^{2+}$ release was measured in presence of 10 $\mu$M $IP_3$ as described in MATERIALS AND METHODS and in legend to Fig. 1. Total ATP concentration was kept at 1 mM, and total $Mg^{2+}$ concentration varied from 0.1 to 3 mM. Typical experiments are shown depicting the extent of $IP_3$-induced $Ca^{2+}$ release from cerebellar $P_3$ (*A*) and $P_2$ (*B*) as a function of free $Mg^{2+}$ concentration. $Mg^{2+}$ concentrations inhibiting $IP_3$-induced $Ca^{2+}$ release by 50% were determined graphically assuming highest amount of $Ca^{2+}$ release as 100%.

sponse; it is evident that $Mg^{2+}$ shifted such a curve to the right. Hill plots of these curves (Fig. 3*C*) allowed determination of $K_m$. $Mg^{2+}$ seemed to be a noncompetitive inhibitor of $IP_3$-induced $Ca^{2+}$ release, since both extent of $Ca^{2+}$ release (Fig. 3*A*) and $K_m$ (Fig. 3*C*) were different. Additionally, the Hill coefficients were 1.5 and 1.6 in the presence of low and high $Mg^{2+}$, respectively, and indicated that $IP_3$-induced $Ca^{2+}$ release was cooperative.

Several parameters of inhibition of $IP_3$-induced $Ca^{2+}$ release by $Mg^{2+}$ are summarized in Table 1. Low free [$Mg^{2+}$], i.e., 28.6 $\mu$M, increased the rate and extent of $Ca^{2+}$ release and decreased the apparent $K_m$ for $IP_3$-

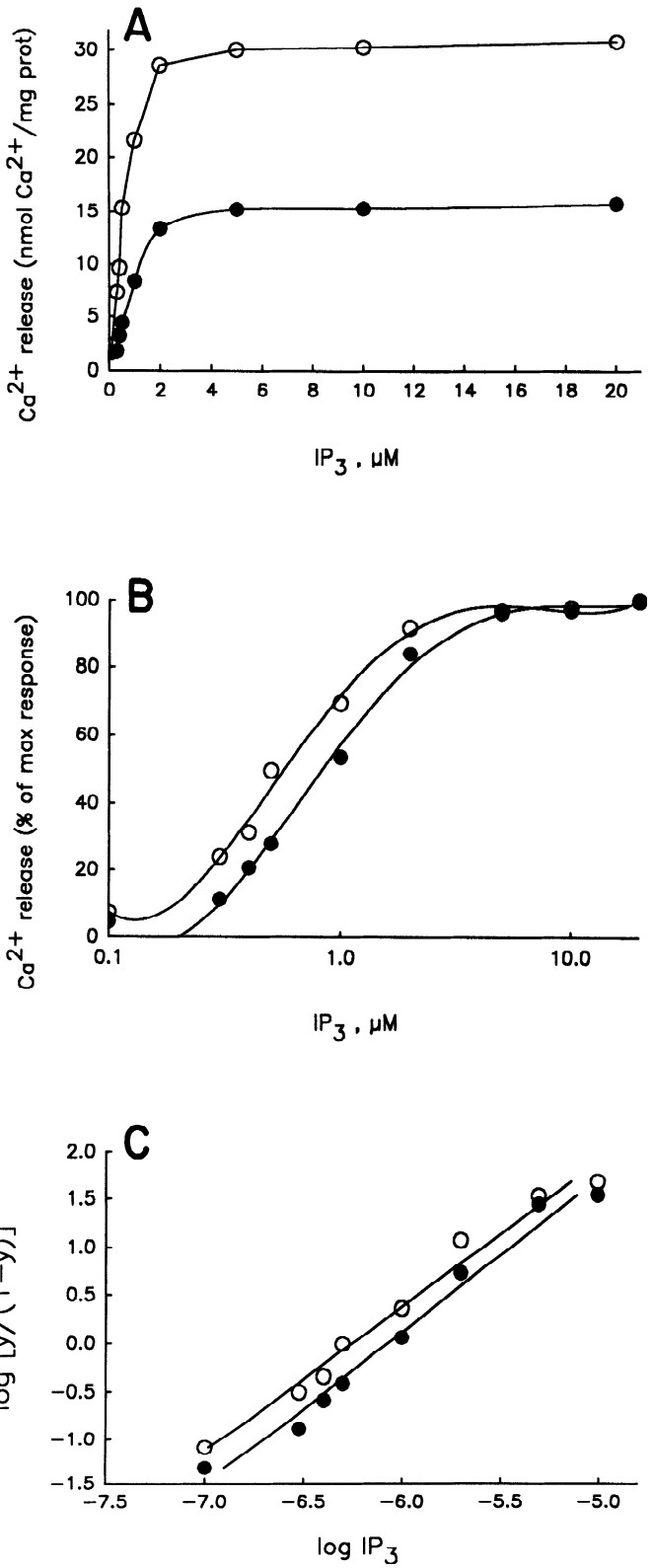


FIG. 3. Influence of $Mg^{2+}$ on dose-response curve for $IP_3$-induced $Ca^{2+}$ release from cerebellar $P_2$ fraction. $IP_3$-induced $Ca^{2+}$ release was measured as described in MATERIALS AND METHODS. $IP_3$ concentration was varied from 0.1 to 20 $\mu$M; total $Mg^{2+}$ concentration was kept either at 0.3 (○) or 2 mM (●). *A*: typical experiment. Extent of $IP_3$-induced $Ca^{2+}$ release is plotted as a function of [$IP_3$]. *B*: extent of $IP_3$-induced $Ca^{2+}$ release is expressed as percentage of maximal response and plotted as a function of [$IP_3$]. *C*: Hill plot of data in *A*. On ordinate, $y$ represents fractional release, which is defined as extent of $Ca^{2+}$ release obtained at a particular $IP_3$ concentration divided by maximal $Ca^{2+}$ release attained over all $IP_3$ concentrations studied. $K_m$ represents the $x$-axis value for $y = 0$. Mean $K_m$ values of several experiments for both $P_2$ and $P_3$ fractions are reported in Table 1.

induced $Ca^{2+}$ release from ~0.9 to 0.4–0.5 $\mu$M $IP_3$. The Hill coefficient was between 1.5 and 1.8 for $P_2$ and $P_3$ fractions, and $Mg^{2+}$ did not affect the degree of cooperativity for $IP_3$-induced $Ca^{2+}$ release. As previously shown (1), cerebellar $P_2$ fractions released larger amounts of accumulated $Ca^{2+}$ as compared with $P_3$ fractions, at both high and low free [$Mg^{2+}$]. No additional insight was gained as to the reasons for different $Ca^{2+}$ release between $P_2$ and $P_3$ fractions (see also Ref. 1).

*$Mg^{2+}$ inhibition of $GPIP_2$-induced $Ca^{2+}$ release.* $Mg^{2+}$-dependent hydrolysis of $IP_3$ might be responsible for some of the differences observed in Fig. 3, particularly at low $IP_3$ concentrations. To address this issue, we repeated experiments reported in Figs. 2 and 3 using $GPIP_2$, a poorly metabolized analogue of $IP_3$ (4, 15, 16). Figure 4*A* shows that $GPIP_2$ induced $Ca^{2+}$ release from cerebellar $P_2$ (Fig. 4*A*, *inset*), although higher concentrations were required to attain maximal $Ca^{2+}$ release (17). $Mg^{2+}$ shifted the dose-response curve for $GPIP_2$-induced $Ca^{2+}$ release to the right; half-maximal release was obtained with 6.5 and 11.8 $\mu$M $GPIP_2$, at 28.6 and 334 $\mu$M free $Mg^{2+}$, respectively. Figure 4*B* shows that $Mg^{2+}$ inhibited $Ca^{2+}$ release elicited by a saturating concentration of $GPIP_2$ (30 $\mu$M) in a concentration-dependent manner. These experiments, together with estimates of $IP_3$ hydrolysis (see above), clearly suggest that inhibition of $IP_3$-induced $Ca^{2+}$ release by $Mg^{2+}$ was not due to augmented $Mg^{2+}$-dependent $IP_3$ hydrolysis.

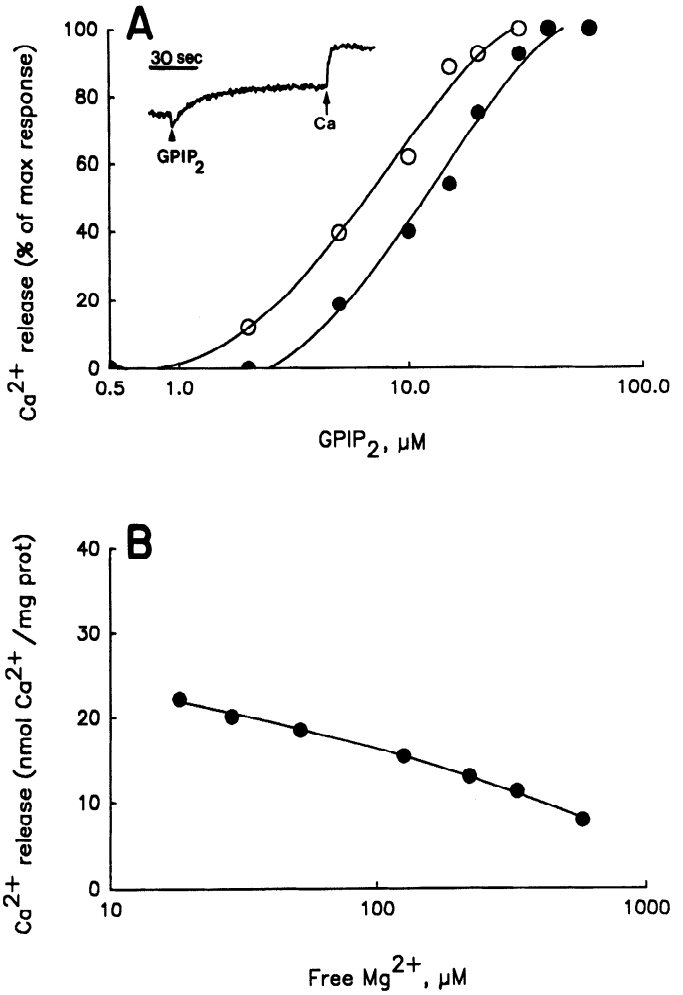


FIG. 4. Effect of $Mg^{2+}$ on glycophosphoinositol 4,5-bisphosphate $GPIP_2$-induced $Ca^{2+}$ release from cerebellar $P_2$ fraction. $Ca^{2+}$ loading of cerebellar $P_2$ fraction (40 nmol $Ca^{2+}$/mg protein) was carried out as described in MATERIALS AND METHODS. *A*: total $Mg^{2+}$ concentration was kept either at 0.3 (○) or 2 mM (●); $GPIP_2$ concentration was varied from 0.1 to 40 $\mu$M. Extent of $GPIP_2$-induced $Ca^{2+}$ release is expressed as percentage of maximal response and is plotted as a function of [$GPIP_2$]. $GPIP_2$ was one order of magnitude less effective than $IP_3$. However, saturating concentrations of either $IP_3$ or $GPIP_2$ released similar amounts of $Ca^{2+}$ (not shown). *Inset*: spectrophotometric tracing in which 30 $\mu$M $GPIP_2$ (arrowhead) was added to cerebellar $P_2$ fraction. Downward deflection at $GPIP_2$ addition is an artifact also observed in absence of membrane protein (not shown). Arrow, addition of 10 nmol $CaCl_2$. *B*: total ATP concentration was kept at 1 mM, and total $Mg^{2+}$ concentration varied from 0.2 to 3 mM. $Ca^{2+}$ release was elicited by adding 30 $\mu$M $GPIP_2$. Extent of $GPIP_2$-induced $Ca^{2+}$ release is plotted as function of free $Mg^{2+}$ concentration.

*Effect of $Mg^{2+}$ on [$^3$H]$IP_3$ binding.* $Mg^{2+}$ was found to be a noncompetitive inhibitor of [$^3$H]$IP_3$ binding by the Scatchard analysis shown in Fig. 5. The plot indicates that 0.5 mM free $Mg^{2+}$ decreased $B_{max}$ from ~10 to 3 pmol [$^3$H]$IP_3$ bound/mg protein and increased $K_d$ from 117 to 171 nM. Mean values of $B_{max}$ and $K_d$ for three different experiments are reported in Table 2. $K_d$ values for [$^3$H]$IP_3$ binding were higher than previously reported (1, 17, 27) because of the presence of 50 mM phosphate, which was added to the assay medium to help inhibit the $IP_3$ase (14). Figure 5, *inset*, shows, however, that in the absence of both $Mg^{2+}$ and 50 mM phosphate, $B_{max}$ was unchanged (~10 pmol [$^3$H]$IP_3$ bound/mg protein) and $K_d$ was in the expected range, i.e., 34.4 nM (compare Refs. 1, 17, 27).

Hill plots of [$^3$H]$IP_3$ binding data (not shown) yielded linear relationships with slopes ~1, which is consistent with a one-site model (24, 27), and indicated that $Mg^{2+}$ did not influence the degree of cooperativity for [$^3$H]$IP_3$

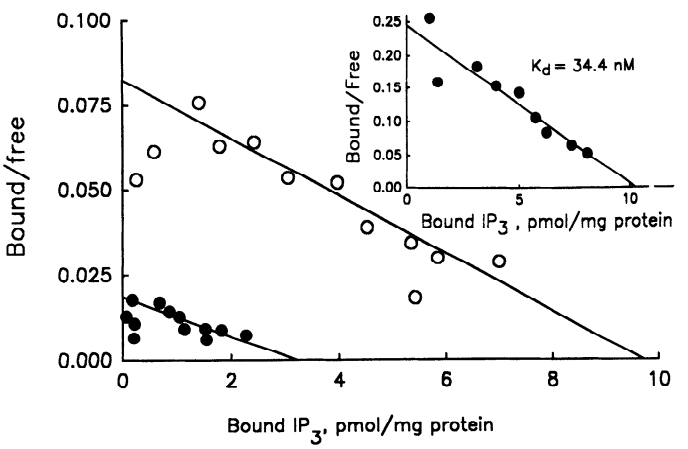


FIG. 5. Effect of 0.5 mM free $Mg^{2+}$ on [$^3$H]$IP_3$ binding to cerebellar $P_2$ fraction. Data are presented as a Scatchard plot analysis for a typical experiment. [$^3$H]$IP_3$ binding was carried out as described in MATERIALS AND METHODS in presence of 50 mM phosphate and in presence (●) or absence (○) of 0.5 mM free $Mg^{2+}$. Phosphate was used to inhibit, at least partially, $IP_3$ase (14). 2,3-Bisphosphoglycerate, a known inhibitor of the $IP_3$ase, was found to inhibit $IP_3$ binding as well (not shown, see also Ref. 27) and could not be used in these experiments. *Inset*: $IP_3$ binding in absence of both 50 mM phosphate and $Mg^{2+}$. Under these experimental conditions $K_d$ was found to be 34.4 nM, similar to that previously reported for either dog (1) or rat (17, 27) cerebellar membrane vesicles.

binding. Mean values for three experiments are reported in Table 2.

*$IP_3$ hydrolysis in [$^3$H]$IP_3$ binding medium.* It would be expected that $IP_3$ase would not be very active in the [$^3$H]$IP_3$ binding medium because of the presence of phosphate, the temperature (1.6°C), and the fact that the $IP_3$ concentrations used were well below the $K_m$ of the $IP_3$ase of ~15 μM (14, 17). Nevertheless, 0.5 mM free $Mg^{2+}$ might promote the action of the $IP_3$ase, and the actual $IP_3$ concentration in the $IP_3$ binding medium might be lower than the nominal one. The extent of $IP_3$ hydrolysis was thus measured by HPLC in the absence and presence of 0.5 mM free $Mg^{2+}$ (Fig. 6). After a 30-min incubation in the absence of $Mg^{2+}$, the cerebellar $P_2$ fraction degraded only 3.8% of the initial 50 nM [$^3$H]$IP_3$ into [$^3$H]-$IP_2$ (Fig. 6, solid line). In the presence of $Mg^{2+}$, 5.1% of the initial [$^3$H]$IP_3$ was hydrolyzed (Fig. 6, dotted line). Using bovine adrenal cortex membranes, Guillemette et al. (14) reported that 9% of the initial $IP_3$ was hydrolyzed after 15-min incubation in the presence of $Mg^{2+}$. If data of Fig. 5 are corrected for the actual $IP_3$ concentrations in the presence and absence of $Mg^{2+}$, both $B_{max}$ and $K_d$ do not change appreciably. Additionally, we could not detect any specific [$^3$H]$IP_2$ binding with 15 nM [$^3$H]$IP_2$ (not shown), which implies that all specific binding was due to [$^3$H]$IP_3$.

*Effect of $Mg^{2+}$ on heparin inhibition of $IP_3$-induced $Ca^{2+}$ release.* Heparin, a competitive inhibitor of $IP_3$-induced $Ca^{2+}$ release (13), was previously found to inhibit $IP_3$-induced $Ca^{2+}$ release from canine brain microsomes (21) with an apparent inhibitory constant ($K_i$) of 14 μM at 127 μM free $Mg^{2+}$. Figure 7*A* shows that 14 μM heparin inhibited $IP_3$-induced $Ca^{2+}$ release from the cerebellar $P_2$ fraction at both low and high free $Mg^{2+}$, i.e., 28.6 and 334 μM $Mg^{2+}$ (Fig. 7, *C* and *D*, respectively). Both the extent and rate of $IP_3$-induced $Ca^{2+}$ release were affected by heparin. Figure 7*B* shows the inhibitory effect of two different heparin concentrations, i.e., 14 and 22 μM, on $IP_3$-induced $Ca^{2+}$ release when free $Mg^{2+}$ varied between 18 and 585 μM. The plot clearly indicates that $Mg^{2+}$ and heparin are additive inhibitors. The Dixon plot of Fig. 7*C* shows that the families of curves intersect below $1/R_{max}$ and above the *x*-axis, as expected for the interaction between a competitive inhibitor (heparin) and a mixed-type inhibitor ($Mg^{2+}$), which are not mutually exclusive. Thus $Mg^{2+}$ and heparin seem to have distinct binding sites.

## DISCUSSION

*Intracellular effects of $Mg^{2+}$.* $Mg^{2+}$ is involved in several aspects of neuronal function (12). It is a cofactor for hundreds of enzymes, plays an important role in protein synthesis, and is also involved in a wealth of metabolic processes, i.e., glycolysis, respiration. Intracellular $Mg^{2+}$ regulates transmembrane transport of ions such as $Na^+$ and $Ca^{2+}$ (2) and may also act as cofactor of ion channels, since $Mg^{2+}$ is the blocking ion producing inward $K^+$ rectification (23).

Very little is known about the free $Mg^{2+}$ concentration in vertebrate neurons and whether the resting free $Mg^{2+}$ concentration changes upon cell activation (2). By $^{31}$P-nuclear magnetic resonance spectra of superfused cerebral tissues, free $Mg^{2+}$ values of 0.33 mM have recently been reported (5). These values were increased by hypoglycemia, hypoxia, or reduced extracellular $Ca^{2+}$ (5). Intracellular free $Mg^{2+}$ seems to be well buffered (2) as measured by $Mg^{2+}$-sensitive microelectrodes, which, however, lack the time resolution required to detect transient changes of free $Mg^{2+}$ concentration. In this respect, monitoring cytoplasmic free $Mg^{2+}$ in cultured neurons loaded with Furaptra, a cell-trappable fluorescent $Mg^{2+}$ indicator (19), should soon provide valuable information.

*Do the present data have physiological relevance?* This paper shows that $Mg^{2+}$ is an in vitro inhibitor of both $IP_3$-induced $Ca^{2+}$ release from isolated cerebellar membrane fractions and [$^3$H]$IP_3$ binding. The present observations indicate that, if the resting intracellular $Mg^{2+}$ concentration is ~0.3 mM (5) and does not change on cell activation, $Mg^{2+}$ controls $IP_3$-induced $Ca^{2+}$ release by affecting both the binding of $IP_3$ to its receptor sites (Fig. 5) and the release of $Ca^{2+}$ via $IP_3$-gated $Ca^{2+}$ channels (Figs. 1–3). A portion of the $IP_3$-sensitive $Ca^{2+}$

TABLE 2. *Effect of $Mg^{2+}$ on [$^3$H]$IP_3$ binding to cerebellar $P_2$ fraction*

| | No $Mg^{2+}$ | 0.5 mM Free $Mg^{2+}$ |
|---|---|---|
| $B_{max}$, pmol/mg protein | 10.9±2.2† | 3.5±0.6† |
| $K_d$, nM | 136±20* | 227±45* |
| Hill coefficient | 1.11±0.15‡ | 1.02±0.08‡ |

Data are means ± SD for 3 different experiments. $B_{max}$, maximal binding; $K_d$, dissociation constant; $IP_3$, inositol 1,4,5-trisphosphate; $P_2$, crude mitochondrial pellet. Experiments were carried out as described in MATERIALS AND METHODS and in legend to Fig. 6. * $P < 0.05$; † $P < 0.01$; ‡ Not significant.

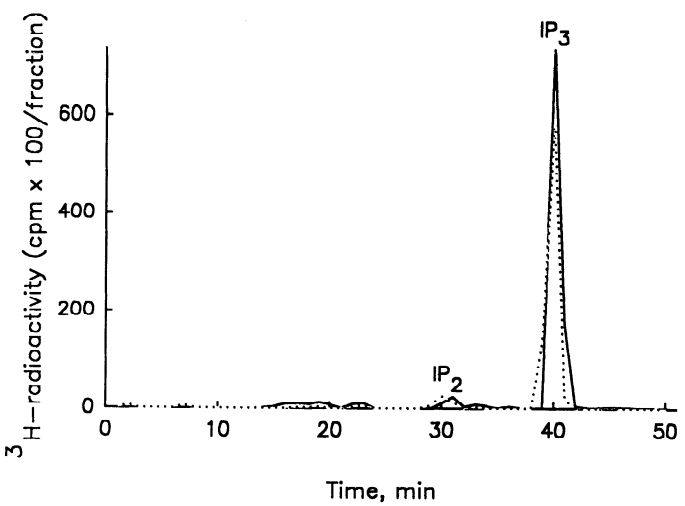


FIG. 6. $IP_3$ hydrolysis by cerebellar $P_2$ fraction in [$^3$H]$IP_3$ binding medium. [$^3$H]$IP_3$ binding media were prepared and high-pressure liquid chromatography (HPLC) analysis carried out as described in MATERIALS AND METHODS. Incubation was performed with 50 nM [$^3$H]$IP_3$ for 30 min at 1.6°C, in presence (dotted line) or absence (solid line) of 0.5 mM free $Mg^{2+}$. Samples were not lyophilized before HPLC separation. Two additional experiments were done in which samples were lyophilized before HPLC separation, and similar results were obtained (not shown). Actual counts (cpm/fraction) referable to [$^3$H]$IP_3$ and [$^3$H]$IP_2$ were 890 × $10^2$ and 35 × $10^2$ and 750 × $10^2$ and 40 × $10^2$, respectively, in absence and presence of $Mg^{2+}$. Data in text are given as $[IP_2/(IP_2 + IP_3)] \times 100$.

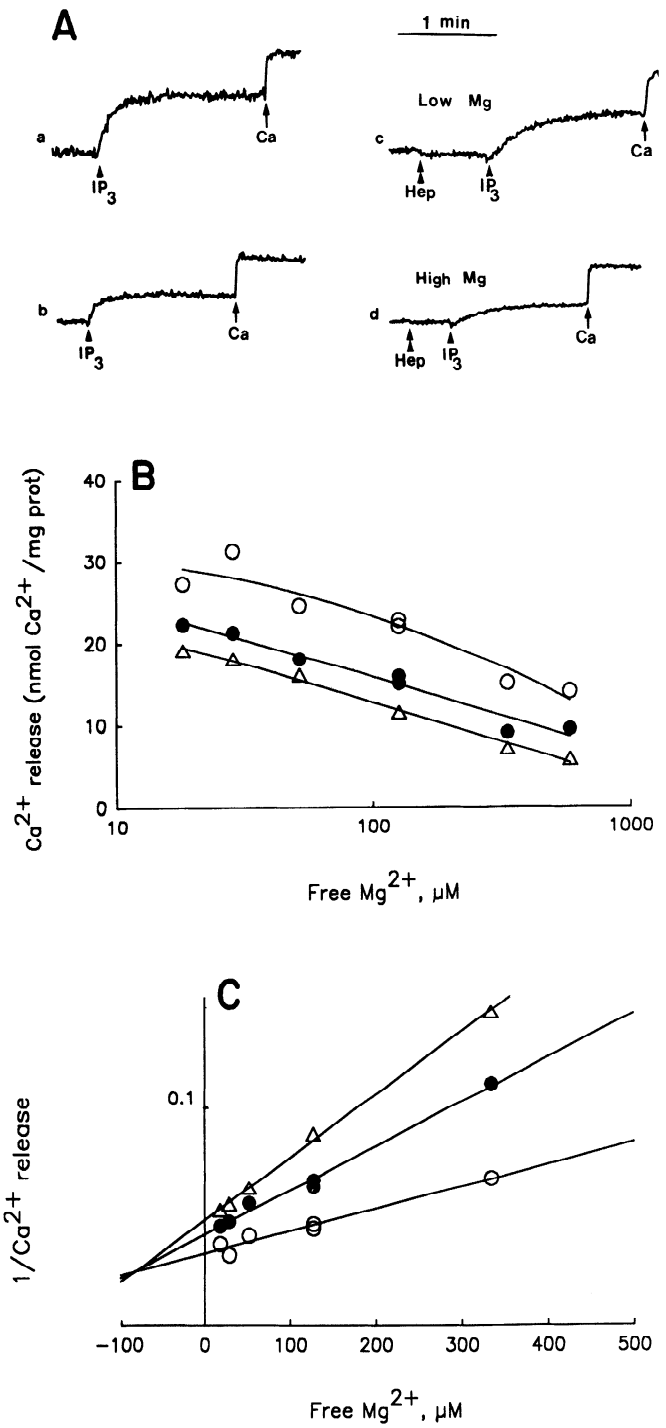


FIG. 7. Effect of heparin and $Mg^{2+}$ on $IP_3$-induced $Ca^{2+}$ release from cerebellar $P_2$ fraction. $Ca^{2+}$ loading and $Ca^{2+}$ release were measured as described in MATERIALS AND METHODS using antipyrylazo III as a $Ca^{2+}$ indicator. *A*: assay was started by adding 0.5 mg of membrane protein and then 2 consecutive 10-nmol $CaCl_2$ pulses (not shown). *Control tracings a* and *b* were in presence of low (*a*) and high (*b*) free $Mg^{2+}$ (28.6 and 334 $\mu$M $Mg^{2+}$, respectively). *Tracings c* and *d*: 14 $\mu$M heparin was added 20–30 s before addition of 10 $\mu$M $IP_3$. *B*: total ATP concentration was kept at 1 mM, and total $Mg^{2+}$ concentration varied from 0.2 to 3 mM. $Ca^{2+}$ release was elicited by adding 10 $\mu$M $IP_3$. Extent of $IP_3$-induced $Ca^{2+}$ release is plotted as function of free $Mg^{2+}$. ○, Control; ●, + 14 $\mu$M heparin; △, plus 22 $\mu$M heparin. Average molecular weight of heparin was assumed to be 5,000 (21). *C*: Dixon plot of data of *B*; symbols are as in *B*.

channels could always be in a closed state provided that other in situ regulatory factors, yet to be identified, do not play opposite roles.

Transient or long-lasting changes (5) of free $Mg^{2+}$ concentration are also expected to affect $IP_3$-induced $Ca^{2+}$ release. During an intracellular $Ca^{2+}$ transient, free $Mg^{2+}$ might increase, at least temporarily, if $Ca^{2+}$ and $Mg^{2+}$ compete for the same cytoplasmic binding sites. The magnitude and duration of free $Mg^{2+}$ change would reflect the kinetics of $Ca^{2+}$ transport back into intracellular $Ca^{2+}$ stores, $Ca^{2+}$ extrusion from the cell, and $Ca^{2+}$ binding to cytoplasmic $Ca^{2+}$-$Mg^{2+}$ binding proteins, e.g., parvalbumin (6). Such an increase of $Mg^{2+}$ concentration would decrease both $IP_3$ binding and $IP_3$-induced $Ca^{2+}$ release. Within this hypothetical scenario, increasing the free $Mg^{2+}$ concentration would favor the formal transition to the closed state of the $IP_3$-gated $Ca^{2+}$ channel.

There is ample evidence that $IP_3$ releases only part, i.e., 30–50%, of the $Ca^{2+}$ accumulated by intracellular high affinity $Ca^{2+}$ stores (17). The present findings indicate that estimates of the $IP_3$-sensitive $Ca^{2+}$ store are influenced by the experimental conditions, notably by the free $Mg^{2+}$ concentration. Data of Table 1 show that $IP_3$ releases part of the actively accumulated $Ca^{2+}$ (40 nmol $Ca^{2+}$/mg protein) and suggest that the size of the $IP_3$-sensitive $Ca^{2+}$ store may vary from 43 to 75% of the total ($IP_3$-sensitive and $IP_3$-insensitive) $Ca^{2+}$ store of the $P_2$ fraction (40 nmol $Ca^{2+}$/mg protein), depending on the $Mg^{2+}$ concentration of the assay medium (see legend to Table 1). An $IP_3$-insensitive $Ca^{2+}$ store can be detected even at low free $Mg^{2+}$ concentrations, although its identification, characteristics, and relationship to the $IP_3$-sensitive $Ca^{2+}$ store are still unknown (see also Ref. 1).

*Mechanism of $Mg^{2+}$ inhibition.* $Mg^{2+}$ is shown to be a noncompetitive inhibitor of both [$^3$H]$IP_3$ binding and $IP_3$-induced $Ca^{2+}$ release. The [$^3$H]$IP_3$ binding data (Fig. 5 and Table 2), even when adjusted for the small amount of $IP_3$ degraded in the presence of 0.5 mM free $Mg^{2+}$ (Fig. 6), clearly indicate the noncompetitive nature of the inhibition. The effect of $Mg^{2+}$ on $IP_3$-induced $Ca^{2+}$ release was studied after active $Ca^{2+}$ preloading and under experimental conditions which necessarily favored $IP_3$ hydrolysis, e.g., micromolar concentrations of $IP_3$, $Mg^{2+}$, and 37°C. We have demonstrated that $Mg^{2+}$ is an inhibitor of $IP_3$-induced $Ca^{2+}$ release by showing that *1)* saturating concentrations of $IP_3$ released less $Ca^{2+}$ at high free $Mg^{2+}$ (Figs. 2 and 3*A*). *2)* $Mg^{2+}$ inhibited $IP_3$- and $GPIP_2$-induced $Ca^{2+}$ release with identical characteristics (Fig. 4). *3)* $Mg^{2+}$ caused a shift to the right of the dose-dependence curve for both $IP_3$- and $GPIP_2$-induced $Ca^{2+}$ release (Figs. 3*B* and 4*A*, respectively). *4)* $Ca^{2+}$ reuptake, after addition of $IP_3$, was similar at low and high free $Mg^{2+}$ concentrations, i.e., 28.6 and 334 $\mu$M, respectively (uptake phases in Fig. 1). *5)* Of the initial concentration, 85–90% of $IP_3$ was left after 20 s, i.e., the time to peak $Ca^{2+}$ release (compare Fig. 1). Thus differences in $K_m$ (Fig. 3*C*) and extent of $IP_3$-induced $Ca^{2+}$ release (Fig. 3*A*) indicate that $Mg^{2+}$ is indeed a noncompetitive inhibitor of $IP_3$-induced $Ca^{2+}$ release.

The effects of $Mg^{2+}$ are different from those exerted by free $Ca^{2+}$ and pH, which change only the apparent affinity of the $IP_3$ receptor of rat cerebellar microsomes

(16). $IP_3$-induced $Ca^{2+}$ release from canine brain microsomes was also shown to be inhibited by increasing free $Ca^{2+}$ (21). Half-maximal inhibition of $IP_3$-induced $Ca^{2+}$ release was obtained at ~6 $\mu$M free $Ca^{2+}$ (21). Previous data (16, 21) and present results, taken together, indicate that the mechanisms of inhibition by $Mg^{2+}$ and $Ca^{2+}$ are different and that the inhibitory site(s) has(have) an apparent affinity for $Ca^{2+}$ (6 $\mu$M) 10-fold higher than for $Mg^{2+}$ (~60 $\mu$M; Fig. 2). It is not known, however, whether $Mg^{2+}$ and $Ca^{2+}$ have distinct binding sites.

Additional insight into the mechanism of action of $Mg^{2+}$ was provided by experiments carried out with heparin, known to be a competitive inhibitor of $IP_3$ binding and $IP_3$-induced $Ca^{2+}$ release (13, 17). Dixon plot analysis of inhibition curves with increasing concentrations of heparin (Fig. 7*C*) clearly shows that $Mg^{2+}$ and heparin, and thus $IP_3$, have distinct binding sites.

The overall effect of $Mg^{2+}$ was to reduce the affinity of the receptor for $IP_3$. The $Mg^{2+}$ effect on the $K_d$ for [$^3$H]$IP_3$ binding and the $K_m$ for $IP_3$-induced $Ca^{2+}$ release seems to be quantitatively different. In the presence of phosphate, the average $K_d$ was 136 nM, and the $K_m$ was 480 nM at low free $Mg^{2+}$; at high free $Mg^{2+}$, the average $K_d$ was 227 nM and the $K_m$ was 940 nM (Tables 1 and 2). It has long been acknowledged that the two constants are different mainly because of the different experimental conditions, e.g., temperature, pH, $IP_3$, and $Mg^{2+}$ concentrations, etc. (17), and the present study is no exception. However, since the $IP_3$ binding has been reported to be noncooperative (24, 27, and Table 2), whereas both the opening of the $Ca^{2+}$ channel (18) and $IP_3$-induced $Ca^{2+}$ release (Fig. 3*C* and Table 1) appear to be cooperative, one should regard $IP_3$ binding as part of, rather than equivalent to, $IP_3$-induced $Ca^{2+}$ release. The $K_d$ and $K_m$ need not necessarily be identical if the channel is a multiprotein complex comprised of, at least, the $IP_3$ receptor, the channel pore, and a $Ca^{2+}$ regulatory protein, i.e., calmedin (7). Differences between $K_d$ and $K_m$ may be present, even though the $IP_3$-binding site and channel pore domains belong to the same polypeptide (10).

$Mg^{2+}$ might have more than one site of action and influence both $IP_3$ binding, as clearly shown here, and $Ca^{2+}$ channel opening. The reduction of $B_{max}$ would indicate that $Mg^{2+}$ decreases the number of activatable $Ca^{2+}$ channels. $Mg^{2+}$ might also interact with the conduction pathway and inhibit $Ca^{2+}$ permeation, as has been suggested for the skeletal muscle sarcoplasmic reticulum $Ca^{2+}$ release channel (22). Single channel analysis of cerebellar vesicles incorporated into planar lipid bilayers and additional kinetic studies of $Ca^{2+}$ release will further clarify the mechanism of action of $Mg^{2+}$ on the $IP_3$-gated $Ca^{2+}$ channel.

We thank Drs. Aileen K. Ritchie and Daniel Lang for comments on the manuscript, Monica "LG" Tzinas for excellent technical assistance, and Lynette Durant for typing the manuscript.

This work was supported by National Institutes of Health Grants GM-40068-02 (to P. Volpe) and HL-37943 (to G. A. Nickols).

Address for reprint requests: P. Volpe, Dept. of Physiology and Biophysics, Univ. of Texas Medical Branch, Galveston, TX 77550.

Received 8 November 1989; accepted in final form 19 January 1990.

REFERENCES

1. ALDERSON, B. H., AND P. VOLPE. Distribution of endoplasmic reticulum and calciosome markers in membrane fractions isolated from different regions of the canine brain. *Arch. Biochem. Biophys.* 272: 164–172, 1989.
2. ALVAREZ-LEEFMANS, F. J., F. GIRALDEZ, AND S. M. GAMIÑO. Intracellular free magnesium in excitable cells: its measurement and its biologic significance. *Can. J. Physiol. Pharmacol.* 65: 915–925, 1987.
3. BERRIDGE, M. J. Inositol trisphosphate and diacylglycerol: two interacting second messengers. *Annu. Rev. Biochem.* 56: 159–193, 1987.
4. BERRIDGE, M. J., M. C. DAWSON, AND C. P. DOWNES, H. P. HESLOP, AND R. F. IRVINE. Changes in the levels of inositol phosphates after agonist-dependent hydrolysis of membrane phosphoinositides. *Biochem. J.* 212: 473–482, 1983.
5. BROOKS, K. J., AND M. S. BACHELARD. Changes in intracellular free magnesium during hypoglycaemia and hypoxia in cerebral tissue as calculated from $^{31}$P-nuclear magnetic resonance spectra. *J. Neurochem.* 53: 331–334, 1989.
6. CELIO, M. R., AND C. W. HEIZMANN. Calcium-binding protein parvalbumin as a neuronal marker. *Nature Lond.* 293: 300–302, 1981.
7. DANOFF, S. K., S. SUPATTAPONE, AND S. H. SNYDER. Characterization of a membrane protein from brain mediating the inhibition of inositol 1,4,5-trisphosphate receptor binding by calcium. *Biochem. J.* 245: 701–705, 1988.
8. DANOFF, S. K., A. THEIBERT, R. EVANS, AND S. H. SNYDER. $Ca^{2+}$-dependent regulation of Ins-1,4,5-$P_3$ binding to rat cerebellar receptor. *Soc. Neurosci. Abstr.* 15: 1004, 1989.
9. EDELMAN, A. M., D. D. HUNTER, A. E. HENDRICKSON, AND E. G. KREBS. Subcellular distribution of calcium- and calmodulin-dependent myosin light chain phosphorylating activity in rat cerebral cortex. *J. Neurochem.* 5: 2603–2617, 1985.
10. FERRIS, C. D., R. L. HUGANIR, S. SUPATTAPONE, AND S. H. SNYDER. Purified inositol 1,4,5-trisphosphate receptor mediates calcium flux in reconstituted lipid vesicles. *Nature Lond.* 342: 87–89, 1989.
11. FISHER, S. K., AND B. W. AGRANOFF. Receptor activation and inositol lipid hydrolysis in neural tissues. *J. Neurochem.* 48: 999–1017, 1987.
12. FLATMAN, P. W. Magnesium transport across cell membranes. *J. Membr. Biol.* 80: 1–14, 1984.
13. GOSH, T. K., P. S. EIS, J. M. MULLANEY, C. J. EBERT, AND D. L. GILL. Competitive, reversible and potent antagonism of inositol 1,4,5-trisphosphate-activated calcium release by heparin. *J. Biol. Chem.* 263: 11075–11079, 1988.
14. GUILLEMETTE, G., T. BALLA, A. J. BAUKAL, AND K. J. CATT. Intracellular receptors for inositol 1,4,5-trisphosphate in angiotensin II target tissues. *J. Biol. Chem.* 262: 1010–1015, 1987.
15. JOSEPH, S. K., AND H. L. RICE. 1989. The relationship between inositol trisphosphate receptor density and calcium release in brain microsomes. *Mol. Pharmacol.* 35: 355–359, 1989.
16. JOSEPH, S. K., H. L. RICE, AND J. R. WILLIAMSON. The effect of external calcium and pH on inositol trisphosphate mediated calcium release from cerebellum microsomal preparations. *Biochem. J.* 258: 261–265, 1989.
17. JOSEPH, S. K., AND J. R. WILLIAMSON. Inositol polyphosphates and intracellular calcium release. *Arch. Biochem. Biophys.* 273: 1–15, 1989.
18. MEYER, T., D. HOLOWKA, AND L. STRYER. Highly cooperative opening of calcium channels by inositol 1,4,5-trisphosphate. *Science Wash. DC* 240: 653–656, 1988.
19. MURPHY, E., C. C. FREUDENRICH, L. A. LEVY, R. E. LONDON, AND M. LIEBERMAN. Monitoring cytosolic free magnesium in cultured chicken heart cells by use of the fluorescent indicator Furaptra. *Proc. Natl. Acad. Sci. USA* 86: 2981–2984, 1989.
20. NAHORSKI, S. R. Inositol polyphosphates and neuronal calcium homeostasis. *Trends Neurosci.* 11: 444–448, 1988.
21. PALADE, P., C. DETTBARN, B. ALDERSON, AND P. VOLPE. Pharmacologic differentiation between inositol 1,4,5-trisphosphate-induced $Ca^{2+}$ release and $Ca^{2+}$- or caffeine-induced $Ca^{2+}$ release from intracellular membrane systems. *Mol. Pharmacol.* 36: 673–680, 1989.

22. SMITH, J. S., R. CORONADO, AND G. MEISSNER. Single channel measurements of the $Ca^{2+}$ release channel from skeletal muscle sarcoplasmic reticulum. *J. Gen. Physiol.* 88: 573–588, 1986.
23. STANFIELD, P. R. Intracellular $Mg^{2+}$ may act as co-factor in ion channel function. *Trends Neurosci.* 11: 474–476, 1988.
24. STAUDERMAN, K. A., G. D. HARRIS, AND W. LOVENBERG. Characterization of inositol 1,4,5-trisphosphate-stimulated calcium release from rat cerebellar microsomal fractions. *Biochem. J.* 255: 677–683, 1988.
25. SUPATTAPONE, S., S. K. DANOFF, A. THEIBERT, S. K. JOSEPH, J. STEINER, AND S. H. SNYDER. Cyclic AMP-dependent phosphorylation of a brain inositol trisphosphate receptor decreases its release of calcium. *Proc. Natl. Acad. Sci. USA* 85: 8747–8750, 1988.
26. VOLPE, P., AND B. H. ALDERSON-LANG. Regulation of inositol 1,4,5-trisphosphate-induced $Ca^{2+}$ release. II. Effect of cAMP-dependent protein kinase. *Am. J. Physiol.* 258 (*Cell Physiol.* 27): C1086–C1091, 1990.
27. WORLEY, P. F., J. M. BARABAN, S. SUPATTAPONE, V. S. WILSON, AND S. H. SNYDER. Characterization of inositol trisphosphate receptor binding in brain. *J. Biol. Chem.* 262: 12132–12136, 1987.